SUBMITTED TO APJL
Preprint typeset using LaTeX style emulateapj v. 08/13/06

DEMOGRAPHICS OF BULGE TYPES WITHIN 11 MPC AND IMPLICATIONS FOR GALAXY EVOLUTION

DAVID B. FISHER[1]
Laboratory of Millimeter Astronomy, University of Maryland, College Park, MD 29742

NIV DRORY[2]
Instituto de Astronomía, Universidad Nacional Autónoma de México, A.P. 70-264, 04510 México, D.F., México
Submitted to ApJL

ABSTRACT

We present an inventory of galaxy bulge types (elliptical galaxy, classical bulge, pseudobulge, and bulgeless galaxy) in a volume-limited sample within the local 11 Mpc volume using Spitzer 3.6 μm and HST data. We find that whether counting by number, star formation rate, or stellar mass, the dominant galaxy type in the local universe has pure disk characteristics (either hosting a pseudobulge or being bulgeless). Galaxies that contain either a pseudobulge or no bulge combine to account for over 80% of the number of galaxies above a stellar mass of 10^9 $M_\odot$. Classical bulges and elliptical galaxies account for $\sim$1/4, and disks for $\sim$3/4 of the stellar mass in the local 11 Mpc. About 2/3 of all star formation in the local volume takes place in galaxies with pseudobulges. Looking at the fraction of galaxies with different bulge types as a function of stellar mass, we find that the frequency of classical bulges strongly increases with stellar mass, and comes to dominate above $10^{10.5}$ $M_\odot$. Galaxies with pseudobulges dominate at $10^{9.5}$-$10^{10.5}$ $M_\odot$. Yet lower-mass galaxies are most likely to be bulgeless. If pseudobulges are not a product of mergers, then the frequency of pseudobulges in the local universe poses a challenge for galaxy evolution models.

Subject headings: galaxies: bulges — galaxies: formation — galaxies: evolution — galaxies: structure — galaxies: fundamental parameters

1. INTRODUCTION

Hierarchical galaxy evolution models (e.g. White & Rees 1978; Cole et al. 1994) rely on the assumption that bulge-to-total ratios increase directly, and exclusively, from merging (reviewed in Baugh 2006). This has been justified by the ability of simulations of mergers to reproduce properties of ellipticals (e.g. Cox et al. 2006; Naab et al. 2006), and the extrapolation motivated by observations of notable galaxies (e.g. M 31) that bulges are similar to ellipticals.

Yet, there is a dichotomy in the properties of bulges and possibly in their formation mechanisms. Some bulges are similar to elliptical galaxies (*classical bulges*), other bulges resemble disks (*pseudobulges*; for reviews see Kormendy & Kennicutt 2004; Combes 2009). Cursory analysis suggests that simulations producing bulge-disk galaxies (e.g. Governato et al. 2009) are likely not making pseudobulges.

Many authors propose that disk-like bulges form through internal secular evolution of the disk (for reviews see Kormendy & Kennicutt 2004; Athanassoula 2005). Fisher & Drory (2008) and Fisher & Drory (2010) show that pseudobulges have Sérsic index $n < 2$ and do not follow projections of the fundamental plane of elliptical galaxies, adding evidence that pseudobulges are physically different from classical bulges (which have $n > 2$) and ellipticals. Fisher et al. (2009) find that pseudobulges typically have high enough star formation rates (SFR) to have built their stellar mass within the typical lifetime of a disk. Furthermore, correlations between bulge and disk properties such as stellar age (Peletier & Balcells 1996) and radial size (Fisher & Drory 2008) may result from a formative link between pseudobulges and their surrounding disk. Indeed, Fisher & Drory (2010) find that the only property that correlates with the half-light radius of pseudobulges is the outer disk scale length.

Heller et al. (2007) show that significant gaseous inflow occurs across the central kpc during bar lifetimes. Bureau & Freeman (1999) show evidence that boxy/peanut shaped bulges are the result of bar-buckling in disks. Boxy bulges are found in over 40% of edge on galaxies Lütticke et al. (2000), thus implying that a significant number of bulges may owe their origin to disk phenomena. We caution that secular evolution and accretion/merging are not mutually exclusive (Bournaud & Combes 2002). Fisher & Drory (2010) find that some pseudobulges ($\lesssim$ 13% of their sample) could house a small classical bulge, and still maintain a low Sérsic index.

How common are pseudobulges? Drory & Fisher (2007) find that classical bulges are exclusively found in red-sequence galaxies, and imply that pseudobulges are at least as common as blue, Sa-Sc galaxies. Kormendy et al. (2010) find that in the local 8 Mpc, 11 of 19 galaxies with $V_c > 150$ km s^{-1} show no evidence for a classical bulge; however, this is a small sample that does not allow to study the mass dependence of the frequency of pseudobulges. Weinzirl et al. (2009) show that traditional semi-analytic models of galaxy formation cannot account for the observed number of small bulges. This discrepancy may be a manifestation of the bulge dichotomy, since pseudobulges are more likely to be in low B/T galaxies (Fisher et al. 2009). However, many pseudobulges have $B/T > 0.2$ (Fisher & Drory 2008, 2010).

In this letter, we study the abundance of pseudobulges and classical bulges in the local universe. We determine bulge-types on a sample including all non-edge-on galaxies having $B < 15$ within 11 Mpc ($M_B < -15.2$) and estimate the dependence of pseudobulge frequency on galaxy mass and SFR.

Electronic address: dbfisher@astro.umd.edu
[1] Department of Astronomy, The University of Texas at Austin, 1 University Station C1400, Austin, Texas 78712
[2] Max-Planck-Institut für Extraterrestrische Physik, Giessenbachstraße, 85748 Garching, Germany

2. METHODS

We select a representative volume-limited sample of non-edge-on ($i < 80°$) galaxies within 11 Mpc from the Kennicutt et al. (2008) survey, complete for spirals to $B = 15$ mag (corresponding to $M_B = -15.2$). We require Galactic latitude $|b| > 20°$. We take B_T values from de Vaucouleurs et al. (1991) and HyperLEDA[3] in order of preference. Since the Kennicutt et al. (2008) sample does not cover early-type galaxies, we add these from Tonry et al. (2001), Tully & Fisher (1988), and HyperLEDA using the same magnitude and Galactic latitude cuts. Because bulge diagnosis is not reliable on edge-on galaxies, we exclude disks with inclination greater than 80°. This selection may overemphasize the number of E-galaxies by 10% as they are not flattened. We adopt distances from Kennicutt et al. (2008) augmenting missing data from Tonry et al. (2001), Tully et al. (2009), and Tully & Fisher (1988). Magnitudes and colors are corrected for extinction (Schlegel et al. 1998) and galaxy inclination in the usual manner. The final sample contains 320 galaxies. The full sample and measured quantities are listed in Table 1.

We decompose the major-axis near-IR surface brightness (SB) profile of 97 bright ($M_B < -16$ mag) and non Sm/Irr galaxies at 3.6 μm (2MASS K-band for 6 galaxies) into a Sérsic-function bulge and exponential outer disk. Non-exponential disk components (e.g. bars and rings) are masked. Most of our decompositions are taken from Fisher & Drory (2010). This analysis has been used in many publications including Fisher & Drory (2008); Kormendy et al. (2009); Fisher & Drory (2010). The Sérsic index, n is used to diagnose bulges into pseudo- ($n < 2$) and classical ($n > 2$) bulges (see Fisher & Drory 2008 for a discussion). For those bulges with $n \sim 2$ we supplement bulge identification with nuclear morphology from HST images. Ellipticals are assigned $B/T = 1$. Galaxies in which the decomposition yields $B/T < 0.01$ are assigned $B/T = 0$ and are called "bulgeless". We determine total luminosity by integrating the near-IR SB profile and convert to stellar mass using RC3 $B-V$ color as described in Fisher et al. (2009), following Bell & de Jong (2001). Seven bright galaxies have no $B-V$ recorded and for these we substitute the average color of their Hubble type.

We assume that the 223 faint ($M_B > -16$ mag) or Sm/Irr galaxies in our sample are bulgeless. Most have no usable near-IR data; we therefore use M_B in conjunction with $B-V$ to determine stellar mass. 123 do not have a measurement of $B-V$ and we again use the mean color of their Hubble type instead. For a handful of galaxies we test this against masses determined from near-IR flux, finding good agreement.

Available means of measuring SFR in our sample include GALEX FUV luminosity, Hα luminosity, and 24 μm dust emission; linear combination of either Hα or UV (unobscured light) with 24 μm (extincted light) being most robust.

In galaxies fainter than $M_B = -16$ mag, Lee et al. (2009) find that the UV SFR is systematically higher than that from other tracers, possibly due to differences in the stellar IMF. Therefore, we calculate the SFR from Hα and FUV according to Kennicutt (1998) and take the higher of the two values.

For 78 of the 97 bright galaxies, we measure the total SFR and the SFR within the central 1 kpc by linearly combining the 24 μm and GALEX FUV data (Leroy et al. 2008; Fisher et al. 2009), $SFR = a \times [L(\mathrm{FUV}) + b \times L(24)]$, where a and b are constants calibrated against Kennicutt et al. (2009). The 19 remaining galaxies lack GALEX data. For 6 of these, we measure SFR by linearly combining 24 μm with total Hα luminosity of Kennicutt et al. (2008), $SFR \propto L(\mathrm{H}\alpha) + a_{24} \times L(24)$, according to Kennicutt et al. (2009). The SFR of the central 1 kpc is measured with 24 μm alone as $SFR \propto L(24)^{0.885}$ following Calzetti et al (2007). Four galaxies have data at 24 μm only; for these we follow Fisher et al. (2009). One galaxy has only Hα and one has only UV data; there we use the single band flux ($SFR \propto L(\mathrm{H}\alpha)$ or $SFR \propto L(\mathrm{FUV})$) following Kennicutt (1998) and we cannot measure the luminosity of the central kpc. Finally, 7 of the bright galaxies have no data available for measuring SFR. The method applied to calculate SFR for each galaxy is noted in Table 1.

Uncertainties in stellar mass and SFR are dominated by the scatter in the calibration of measured fluxes to physical quantities. The calibration error for stellar mass is 0.12 dex for near-IR flux and 0.16 dex for M_B. The calibration error for SFR is roughly 15% for data combining Hα+24 μm and FUV+24 μm, and is closer to 20% for data using FUV or Hα.

3. RESULTS

Before discussing our results, we call attention to the environmental bias inherent in studying galaxies in the local 11-Mpc volume due to the low density of that region (reviewed in Peebles & Nusser 2010). For comparison, Kormendy et al. (2009) finds that 2/3 of all stellar mass in the Virgo cluster is in elliptical galaxies alone.

Bulge number statistics: Galaxies with either a pseudobulge or no bulge are the most common among bright galaxies. Restricting ourselves to galaxies more massive than 10^9 $M_\odot$, we find that only 17±10% are galaxies with an observed classical bulge (including elliptical galaxies), 45±12% are galaxies with pseudobulges, 35±12% are are disk galaxies with $B/T < 0.01$, and under 3% are galaxies currently undergoing major merging (NGC 4490, NGC 1487, NGC 2537). Quoted errors are Poisson uncertainties. Dwarf and Irregular galaxies comprise ∼70% of all galaxies having stellar mass lower than 10^9 $M_\odot$ within 11 Mpc. However, they only account for ∼2% of the stellar mass in the same volume.

Star formation in bulge-disk galaxies: 61% of the star formation (SF) in the local 11 Mpc is in galaxies with pseudobulges. A non-negligible 13% of the total SF in our volume occurs in the central kpc of bulge-disk galaxies. Fig. 1 shows the distribution of SFR surface densities (Σ_{SF}) of entire galaxies and the central kpc of bulge-disk galaxies. It is clear that high Σ_{SF} in the central kpc of bulge-disk galaxies is extremely common when compared to global SFR densities. In our sample, we find that 46±9% of galaxies with bulge-to-total ratios in the range $0.01 \leq B/T < 1$ have $\Sigma_{\mathrm{SF}} > 10^{-2} M_\odot$ yr^{-1}kpc^{-2}; only 33±9% of entire galaxies have $\Sigma_{\mathrm{SF}} > 10^{-2} M_\odot$ yr^{-1}kpc^{-2} inside the optical radius. In the bulge sample, 11 bulges do not have data to determine the SFR. If these have low SFR, the fraction of bulges with high Σ_{SF} decreases to 35±10%.

Stellar masses: Fig. 2 shows the stellar-mass distribution of galaxies with pseudobulges, classical bulges and ellipticals (combined), bulgeless galaxies, and the whole sample. Bulgeless galaxies tend to be lower in mass, and dominate the distribution up to $M_* \sim 10^{9.5}$ $M_\odot$. Pseudobulges dominate intermediate mass range from, $M_* \gtrsim \times 10^{9.5}$ to $10^{10.5}$ $M_\odot$. Classical bulges tend to be in more massive galaxies. Galaxies with either a pseudobulge or no bulge combine to account for 56±12% of the stellar mass of galaxies within 11 Mpc. Finally, we calculate the total mass in classical bulges by using the B/T from the bulge-disk decompositions. These values

[3] http://leda.univ-lyon1.fr/

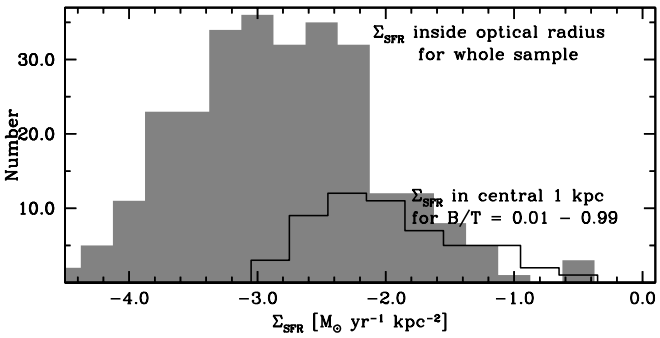

FIG. 1.— The distribution of SFR density $\Sigma_{SF}(r < 1$ kpc) for bulges (black line). For comparison, we also show the SFR density of entire galaxies (Σ_{SF}(total); grey shaded region).

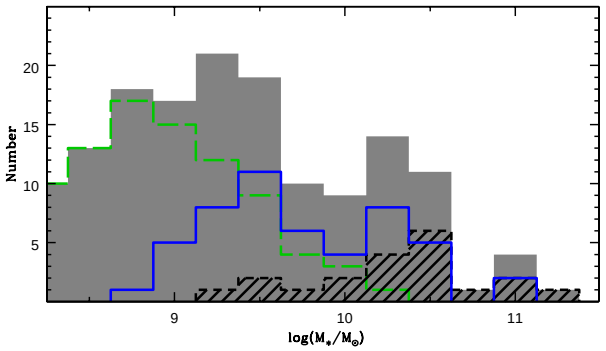

FIG. 2.— The distribution of galaxy stellar mass in galaxies with pseudobulges (blue line), elliptical galaxies and galaxies with classical bulges (short-dashed line), bulgeless galaxies (green long-dashed line) and the full sample (grey shaded region). Note the full range of stellar masses in our sample is not shown.

should be treated as estimates, since they assume the same M/L for both the bulge and disk, hence likely underestimating the classical bulge mass. Classical bulges and E galaxies account for $\sim$1/4 of the stellar mass in the local 11 Mpc, disks account for $\sim 3/4$ of the stellar mass.

4. DISCUSSION

We show that galaxies with pseudobulges are the most common type of bright galaxy in the local 11 Mpc volume. The set of galaxies including pseudobulge and bulgeless galaxies account for just over 1/2 of the mass in stars in the local volume. Roughly $2/3$ of new stars are made in galaxies with pseudobulges. Whether counting by number, mass, or by present-day star formation, the dominant mode of galaxy evolution in the present day local universe is that which occurs in galaxies without classical bulges. These results are therefore in agreement with the observed correlation of bulge type with galaxy properties such as color (Drory & Fisher 2007).

We find that classical bulges and elliptical galaxies combined account for $\sim$1/4 of the stellar mass within 11 Mpc. Therefore, 3/4 of the stellar mass in the local 11 Mpc is in disks (combining all mass in pseudobulges, disks around classical bulges and pseudobulges, and bulgeless galaxies). Recall that in cluster environments, 2/3 of the stellar mass is in elliptical galaxies alone (Kormendy et al. 2009). Thus the process driving the distribution of bulge types appears to be a strong function of environment.

We show that in the majority of bulge-disk galaxies, the central kpc has high SFR surface density (compared to the SFR density for entire galaxies). If a merger drives enhanced SFR for 1 Gyr (Cox et al. 2008), and if fewer than 10% of giant galaxies experience merging each Gyr (e.g. Jogee et al. 2009), then episodic SF can not account for the frequency of enhanced SF observed in our sample, and thus the SF in the centers of (pseudo)bulges is not likely episodic or merger driven. The frequency of enhanced SF in bulges is thus further evidence that bulges are generating new stars through long term, non-episodic processes.

Finally, in Fig. 3, we estimate the relative frequency of classical bulges (including elliptical galaxies), pseudobulges, all bulges, and galaxies with no bulge within 11 Mpc as a function of galaxy stellar mass. To account for the possibility of composite systems, we estimate an upper bound for the frequency of classical bulges: we include all those bulges that satisfy the criteria to be called classical and elliptical galaxies, add all galaxies presently in strong interactions (NGC 4490, NGC 1487, NGC 2537 & NGC 5194A & B), and we estimate the possible number of galaxies with composite (pseudo+classical) bulges. Fisher & Drory (2010) find that models of bulges in which the total bulge light is composed of a high and low Sérsic index component are not inconsistent with decompositions of real bright low-specific-SFR pseudobulges. Consistent with these results, we select all pseudobulges with stellar mass $M_{\rm pseudo} > 10^9$ M$_\odot$ and specific SFR < 0.03 Gyr^{-1} as candidate composite bulges. For the interacting galaxies we make the assumption that a merger will result in an elliptical and thus $B/T = 1$.

Fig. 3 shows that the frequency of pseudobulges and classical bulges in the local universe is strongly dependent on galaxy mass. Pure disk galaxies and those galaxies with pseudobulges are the most common type of galaxy for stellar mass $M_* \leq 10^{10}$ M$_\odot$. Elliptical galaxies and galaxies with classical bulges are the majority of galaxies with $M_* \geq 10^{10.5}$ M$_\odot$. However, since galaxies with $M_* \geq 10^{10.5}$ M$_\odot$ only make up 4% of bright galaxies in the local volume, galaxies with pseudobulges and those with no bulge remain the dominant type of bright galaxy by number. Dynamical evidence suggest that the Milky Way (not included in the sample) does not contain a classical bulge (Shen et al. 2010), its stellar mass places it right at the transition, $M_{*,MW} \sim 10^{10.5}$ M$_\odot$. Therefore, the massive galaxies in the Local Group comprise a pseudobulge galaxy (Milky Way), a classical bulge galaxy (M 31), and a bulgeless disk galaxy (M 33).

The simulation of the evolution of galaxies in a ΛCDM-universe by Croft et al. (2009) provides a good model for comparison. As is normally the case, in this simulation B/T is only increased through the merging process. They find that in massive galaxies ($\gtrsim 10^9$ M$_\odot$) located in low density environments (i.e. field galaxies), 40-50% are bulge-dominated (B/T>80%). In the local 11 Mpc only 23$\pm$5% of galaxies contain classical bulges at any bulge-to-total ratio (including ellipticals and ongoing mergers), and only 5% have B/T>80%. If we assume that the simulation in Croft et al. (2009) only produces classical bulges, then the number of classical bulges in the local universe is much smaller than in a typical galaxy evolution simulation.

Recently, Hopkins et al. (2009b) show that if B/T is a function of both merger mass-ratio and gas fraction in the progenitive merger, then the distribution of B/T for all galaxies is recovered. However, this agreement relies entirely on the interpretation of pseudobulges as merger products (contrary to ob-

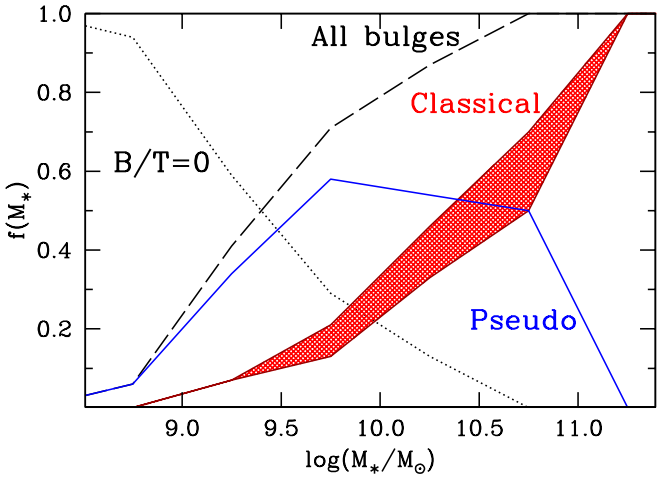

FIG. 3.— The relative number of galaxies with classical bulges and elliptical galaxies (red lines), galaxies containing pseudobulges (blue line), all disk-bulge galaxies (black dashed line), and bulgeless galaxies (black dotted line) as a function of galaxy stellar mass.

servational evidence). In our sample, the fraction of classical-bulge light in galaxies less massive than $M_* \sim 10^{10}$ $M_\odot$ is very low, $B/T \lesssim 5\%$. If pseudobulges are not merger products, but rather disk components, then models continue to produce too much mass in bulges.

We conclude that pseudobulges and internal bulge growth through SF is present in the majority of giant disk galaxies in the local 11 Mpc volume. If we make the assumption that pseudobulges are not direct merger products, then the number of pseudobulges poses a challenge for models of galaxy evolution. Given that very old stellar populations are commonly observed in spiral galaxies (MacArthur et al. 2009), holding off disk galaxy formation until lower redshifts does not appear to be the solution. The problem is that, *as we understand them now*, mergers in recent epochs are likely to increase B/T and heat the disk thereby reducing the secular inward flow of gas in disks, and possibly destroying a pre-existing pseudobulge in a disk galaxy. Therefore, either the merging process does not disrupt disks as easily as simple calculations suggest (see Hopkins et al. 2009a; Moster et al. 2010), or there are fewer galaxy mergers in recent epochs in the universe than simulations suggest.

DBF acknowledges support from University of Maryland, as well as J Kormendy and the University of Texas at Austin. ND and DBF thank the Max-Planck Society for support during this project. We also wish to thank Shardha Jogee, Karl Gebhardt, Neal Evans, John Kormendy and Ralf Bender for their helpful comments and support during the writing of this work. This work is based on observations made with the Spitzer Space Telescope, which is operated by the Jet Propulsion Laboratory, California Institute of Technology under a contract with NASA. Support for this work was provided by NASA through an award issued by JPL/Caltech. DBF acknowledges support by the National Science Foundation under grant AST 06-07490. Some of the data presented in this paper were obtained from the Multi-mission Archive at the Space Telescope Science Institute (MAST). STScI is operated by the Association of Universities for Research in Astronomy, Inc., under NASA contract NAS5-26555. Support for MAST for non-HST data is provided by the NASA Office of Space Science via grant NAG5-7584 and by other grants and contracts.

REFERENCES

Athanassoula, E. 2005, MNRAS, 358, 1477
Baugh, C. M. 2006, Reports on Progress in Physics, 69, 3101
Bell, E. F., & de Jong, R. S. 2001, ApJ, 550, 212
Bournaud, F., & Combes, F. 2002, A&A, 392, 83
Bureau, M., & Freeman, K. C. 1999, AJ, 118, 126
Calzetti et al. 2007, ApJ, 666, 870
Cole, S., Aragon-Salamanca, A., Frenk, C. S., Navarro, J. F., & Zepf, S. E. 1994, MNRAS, 271, 781
Combes, F. 2009, ArXiv e-prints
Cox, T. J., Jonsson, P., Primack, J. R., & Somerville, R. S. 2006, MNRAS, 373, 1013
Cox, T. J., Jonsson, P., Somerville, R. S., Primack, J. R., & Dekel, A. 2008, MNRAS, 384, 386
Croft, R. A. C., Di Matteo, T., Springel, V., & Hernquist, L. 2009, MNRAS, 400, 43
de Vaucouleurs, G., de Vaucouleurs, A., Corwin, Jr., H. G., Buta, R. J., Paturel, G., & Fouque, P. 1991, Third Reference Catalogue of Bright Galaxies (Volume 1-3, XII, 2069 pp. 7 figs.. Springer-Verlag Berlin Heidelberg New York)
Drory, N., & Fisher, D. B. 2007, ApJ, 664, 640
Fisher, D. B., & Drory, N. 2008, AJ, 136, 773
—. 2010, ApJ, 716, 942
Fisher, D. B., Drory, N., & Fabricius, M. H. 2009, ApJ, 697, 630
Governato, F., Brook, C. B., Brooks, A. M., Mayer, L., Willman, B., Jonsson, P., Stilp, A. M., Pope, L., Christensen, C., Wadsley, J., & Quinn, T. 2009, MNRAS, 398, 312
Heller, C. H., Shlosman, I., & Athanassoula, E. 2007, ApJ, 671, 226
Hopkins, P. F., Cox, T. J., Younger, J. D., & Hernquist, L. 2009a, ApJ, 691, 1168
Hopkins, P. F., Somerville, R. S., Cox, T. J., Hernquist, L., Jogee, S., Kereš, D., Ma, C., Robertson, B., & Stewart, K. 2009b, MNRAS, 397, 802
Jogee et al. 2009, ApJ, 697, 1971
Kennicutt, R. C., Hao, C., Calzetti, D., Moustakas, J., Dale, D. A., Bendo, G., Engelbracht, C. W., Johnson, B. D., & Lee, J. C. 2009, ApJ, 703, 1672
Kennicutt, Jr., R. C. 1998, ARA&A, 36, 189
Kennicutt, Jr., R. C., Lee, J. C., Funes, José G., S. J., Sakai, S., & Akiyama, S. 2008, ApJS, 178, 247
Kormendy, J., Drory, N., Bender, R., & Cornell, M. E. 2010, ApJ, 723, 54
Kormendy, J., Fisher, D. B., Cornell, M. E., & Bender, R. 2009, ApJS, 182, 216
Kormendy, J., & Kennicutt, R. C. 2004, ARA&A, 42, 603
Lee, J. C., Gil de Paz, A., Tremonti, C., Kennicutt, R. C., Salim, S., Bothwell, M., Calzetti, D., Dalcanton, J., Dale, D., Engelbracht, C., Funes, S. J. J. G., Johnson, B., Sakai, S., Skillman, E., van Zee, L., Walter, F., & Weisz, D. 2009, ApJ, 706, 599
Leroy, A. K., Walter, F., Brinks, E., Bigiel, F., de Blok, W. J. G., Madore, B., & Thornley, M. D. 2008, AJ, 136, 2782
Lütticke, R., Dettmar, R., & Pohlen, M. 2000, A&AS, 145, 405
MacArthur, L. A., González, J. J., & Courteau, S. 2009, MNRAS, 395, 28
Moster, B. P., Macciò, A. V., Somerville, R. S., Johansson, P. H., & Naab, T. 2010, MNRAS, 403, 1009
Naab, T., Khochfar, S., & Burkert, A. 2006, ApJ, 636, L81
Peebles, P. J. E., & Nusser, A. 2010, ArXiv e-prints
Peletier, R. F., & Balcells, M. 1996, AJ, 111, 2238
Schlegel, D. J., Finkbeiner, D. P., & Davis, M. 1998, ApJ, 500, 525
Shen, J., Rich, R. M., Kormendy, J., Howard, C. D., De Propris, R., & Kunder, A. 2010, ApJ, 720, L72
Tonry, J. L., Dressler, A., Blakeslee, J. P., Ajhar, E. A., Fletcher, A. B., Luppino, G. A., Metzger, M. R., & Moore, C. B. 2001, ApJ, 546, 681
Tully, R. B., & Fisher, J. R. 1988, Catalog of Nearby Galaxies (Catalog of Nearby Galaxies, by R. Brent Tully and J. Richard Fisher, pp. 224. ISBN 0521352991. Cambridge, UK: Cambridge University Press, April 1988.)
Tully, R. B., Rizzi, L., Shaya, E. J., Courtois, H. M., Makarov, D. I., & Jacobs, B. A. 2009, AJ, 138, 323
Weinzirl, T., Jogee, S., Khochfar, S., Burkert, A., & Kormendy, J. 2009, ApJ, 696, 411
White, S. D. M., & Rees, M. J. 1978, MNRAS, 183, 341

TABLE 1
SAMPLE DATA

Galaxy Name	Category [a]	T	Dist. (Mpc)	M_B (mag)	$\log(M_{*,total})$ ($M_\odot$)	$\log(\psi_{total})$ ($M_\odot$ yr^{-1})	SFR Method	B/T	Sérsic index	$\log(\psi_{1\ kpc})$ ($M_\odot$ yr^{-1})
NGC6744	C	4	9.4	-21.2	10.36	-0.27	UV,24	0.15	3.2 ± 1.1	-2.33
NGC0224	C	3	0.8	-21.2	10.62	-1.85	24	0.48	2.1 ± 0.5	-2.04
NGC5194	P[b]	4	8.0	-21.2	10.93	0.35	UV,24	0.11	0.5 ± 0.3	-0.83
NGC4594	C	1	9.3	-21.1	10.96	-0.70	UV,24	0.51	6.2 ± 0.6	-1.51
NGC4258	C[c]	4	8.0	-21.0	10.49	...	...	0.11	2.8 ± 0.6	...
NGC4490	M	7	8.0	-20.9	10.14	-0.36	UV,24	1.00	...	...
NGC3627	P	3	10.1	-20.9	10.54	0.05	UV,24	0.10	1.4 ± 0.7	-0.91
NGC2903	P	4	8.9	-20.9	10.29	0.04	UV,24	0.10	0.5 ± 0.1	-0.39
NGC0253	P	5	3.2	-20.9	10.62	0.22	UV,24	0.05	1.5 ± 0.6	-0.20
NGC5457	P	6	6.7	-20.8	10.24	0.33	UV,24	0.02	1.5 ± 1.8	-1.51
NGC5236	P	5	4.5	-20.7	10.22	0.20	UV,24	0.09	0.4 ± 0.1	-0.15
NGC3031	C	2	3.6	-20.7	10.66	-0.85	UV,24	0.37	3.9 ± 0.5	-1.67
NGC4826	C[c]	2	7.5	-20.6	10.56	-0.48	UV,24	0.29	3.6 ± 0.7	-0.72
NGC1291	C	0	9.4	-20.5	10.98	-0.34	UV,24	0.47	2.7 ± 0.8	-0.92
NGC5055	P	4	7.5	-20.5	10.48	-0.10	UV,24	0.19	1.3 ± 1.4	-1.19
NGC3368	P	2	10.5	-20.4	10.49	-0.69	UV,24	0.26	1.6 ± 0.4	-1.39
NGC4559	nb/d	6	9.7	-20.3	10.34	-0.15	UV,24	0.00	...	...
NGC3521	C	4	8.0	-20.3	10.51	-0.13	UV,24	0.12	2.6 ± 1.6	-1.20
NGC3556	P[d]	6	10.4	-20.1	10.23	...	...	0.21	2.1 ± 1.1	...
NGC3034	nb/d	7	3.5	-20.1	10.04	-0.03	Ha	0.00	...	...
NGC3621	P[d]	7	6.6	-20.0	10.37	-0.40	UV,24	0.01	2.8 ± 1.0	-1.54
NGC0925	P	7	9.2	-20.0	9.53	-0.45	UV,24	0.07	0.7 ± 0.6	-1.47
NGC3379	E	-5	10.5	-20.0	11.18	-1.53	UV,24	1.00	...	...
NGC0628	P	5	7.3	-20.0	9.87	-0.35	UV,24	0.08	1.6 ± 0.3	-1.76
NGC3351	P	3	10.0	-19.9	10.29	-0.16	UV,24	0.16	1.5 ± 0.4	-0.45
NGC4736	P	2	4.7	-19.8	10.27	-0.59	UV,24	0.36	1.3 ± 0.4	-0.99
NGC3623	P	1	7.3	-19.7	10.95	-0.86	UV,24	0.16	1.8 ± 0.8	-2.15
NGC3675	P	3	10.6	-19.6	10.32	-0.53	UV,24	0.14	1.6 ± 1.3	-1.23
NGC4096	P	5	8.3	-19.6	10.12	-0.75	UV,24	0.08	0.8 ± 0.4	-1.57
NGC2403	P	6	3.2	-19.4	9.43	-0.65	UV,24	0.07	0.7 ± 0.7	-1.85
NGC5195	P[b]	2	8.0	-19.3	10.46	-0.50	Ha,24	0.29	1.6 ± 0.3	-0.49
NGC4236	P	8	4.5	-19.2	9.27	-1.00	UV,24	0.01	1.9 ± 0.8	-2.40
NGC0247	nb/d	7	3.7	-19.2	8.59	-0.71	UV,24	0.00	...	...
NGC6684	C	-2	10.9	-19.2	10.13	-1.55	24	0.38	3.5 ± 0.8	-0.49
NGC1512	P	1	9.6	-19.2	9.93	-0.84	UV,24	0.28	1.8 ± 1.2	-1.38
NGC7713	P	7	9.3	-19.1	9.63	-0.50	Ha,24	0.01	1.1 ± 1.9	-1.65
NGC1313	nb/d	7	4.2	-19.1	9.49	-0.46	UV,24	0.00	...	...
NGC0672	nb/d	6	7.2	-18.9	9.05	-1.11	UV,24	0.00	...	...
NGC3377	E	-5	9.3	-18.9	10.47	-2.15	UV,24	1.00	...	...
NGC0598	P	6	0.8	-18.9	9.21	-0.91	UV,24	0.03	1.4 ± 2.3	-1.84
NGC5068	nb/d	6	6.2	-18.9	9.11	-0.89	UV,24	0.00	...	...
NGC3486	P	5	8.2	-18.8	9.42	-0.58	UV,24	0.10	1.6 ± 1.1	-2.04
NGC3344	C	4	6.6	-18.8	9.51	-0.71	UV,24	0.08	2.3 ± 0.6	-1.59
NGC7793	P	7	3.9	-18.8	9.83	-0.60	UV,24	0.02	1.1 ± 0.8	-1.77
NGC3412	C	-2	10.4	-18.8	9.92	-2.15	UV,24	0.39	2.6 ± 0.6	-2.39
NGC6503	P	6	5.3	-18.7	9.46	-1.07	UV,24	0.01	1.0 ± 1.5	-1.65
IC5332	P	7	9.5	-18.7	9.91	-0.37	Ha,24	0.04	1.3 ± 0.6	-2.12
NGC1744	nb/d	6	7.7	-18.7	9.43	-0.92	UV,24	0.00	...	...
NGC4314	P[d]	1	9.7	-18.6	9.85	-1.16	UV,24	0.22	3.1 ± 0.9	-1.22
NGC4605	nb/d	5	5.5	-18.6	9.24	-0.87	UV,24	0.00	...	...
NGC4618	P	8	7.8	-18.6	9.68	-0.86	UV,24	0.04	1.4 ± 1.8	-1.90
NGC1058	P	5	9.2	-18.6	9.21	-0.82	UV,24	0.03	1.5 ± 0.7	-1.79
NGC1156	nb/d	10	7.8	-18.6	8.92	-0.37	UV	0.00	...	...

TABLE 1 — *Continued*

Galaxy Name	Category [a]	T	Dist. (Mpc)	M_B (mag)	$\log(M_{*,\mathrm{total}})$ ($M_\odot$)	$\log(\psi_{\mathrm{total}})$ ($M_\odot$ yr^{-1})	SFR Method	B/T	Sérsic index	$\log(\psi_{1\ \mathrm{kpc}})$ ($M_\odot$ yr^{-1})
NGC1637	P	5	8.9	-18.5	9.53	-0.48	24	0.06	1.1 ± 0.4	-0.68
NGC2787	C	0	7.5	-18.3	10.43	-1.74	UV,24	0.58	2.6 ± 0.5	-1.87
NGC3239	nb/d	9	8.3	-18.3	9.25	-0.51	Ha	0.00	...	...
UGCA90	P	7	10.4	-18.3	9.43	-0.53	UV	0.04	0.9 ± 0.9	...
NGC0024	nb/d	5	8.1	-18.2	9.73	-1.10	UV,24	0.00	...	...
NGC4448	P	2	9.7	-18.2	9.84	-1.28	UV,24	0.17	1.2 ± 0.9	-1.82
NGC0045	nb/d	8	7.1	-18.2	9.94	-0.44	UV,24	0.00	...	...
NGC5474	nb/d	6	7.2	-18.2	9.31	-0.52	UV	0.00	...	...
NGC6689	P	6	9.8	-18.2	9.64	-1.03	Ha,24	0.04	1.2 ± 1.0	-1.32
NGC0949	P	4	9.2	-18.1	9.18	0.00	...	0.20	1.6 ± 1.2	...
NGC6673	P	-1	10.9	-18.1	10.05	...	...	0.29	1.1 ± 0.8	...
NGC0300	nb/d	7	2.0	-18.1	9.20	-0.98	UV,24	0.00	...	...
NGC4242	nb/d	8	7.4	-18.1	10.14	-1.24	UV,24	0.00	...	...
LMC	nb/d	9	0.1	-18.1	9.20	-0.61	Ha	0.00	...	...
NGC4136	P	5	9.7	-18.0	9.01	-1.04	UV,24	0.02	1.8 ± 1.5	-2.19
UGCA114	nb/d	7	9.8	-17.9	9.60	-0.41	UV	0.00	...	...
NGC5585	P	7	5.7	-17.8	9.28	-1.09	UV,24	0.05	0.9 ± 0.3	-2.06
NGC1796	nb/d	5	10.3	-17.8	9.43	-0.49	Ha,24	0.00	...	...
NGC4245	P	0	9.7	-17.8	10.21	-1.76	UV,24	0.21	1.0 ± 0.6	-1.96
NGC2976	nb/d	5	3.6	-17.7	9.53	-1.40	UV,24	0.00	...	...
NGC3077	nb/d	6	3.8	-17.7	9.65	-1.12	Ha	0.00	...	...
NGC4534	nb/d	8	10.8	-17.7	9.02	-0.66	UV	0.00	...	...
NGC5102	C	-3	3.4	-17.6	9.25	...	...	0.37	3.5 ± 0.9	...
NGC5253	nb/d	10	3.2	-17.6	8.87	-0.76	Ha	0.00	...	...
NGC0959	nb/d	8	9.2	-17.6	9.38	-1.34	UV,24	0.00	...	...
NGC1487	M	7	9.1	-17.5	9.39	-0.81	UV,24	1.00	...	...
NGC5949	nb/d	4	8.5	-17.4	9.61	-1.51	UV,24	0.00	...	...
NGC2552	nb/d	9	7.7	-17.4	9.25	-1.52	UV,24	0.00	...	...
IC4710	nb/d	9	7.7	-17.4	9.27	-1.24	UV,24	0.00	...	...
NGC4214	P	9	2.9	-17.4	8.97	-0.96	UV,24	0.01	1.4 ± 1.1	-1.20
NGC2500	P	7	7.6	-17.4	9.42	-1.22	UV,24	0.02	1.7 ± 1.5	-2.13
NGC4941	P	2	6.4	-17.4	9.33	-1.25	UV,24	0.16	1.9 ± 0.7	-1.65
NGC3593	P	0	6.5	-17.3	9.70	-0.86	UV,24	0.51	0.8 ± 0.2	-0.94
NGC4485	nb/d	10	7.1	-17.3	8.76	-0.66	UV	0.00	...	...
NGC3274	nb/d	8	9.5	-17.3	8.94	-1.13	UV,24	0.00	...	...
NGC4020	nb/d	7	9.7	-17.3	9.32	-1.45	UV,24	0.00	...	...
ESO305-G009	nb/d	8	10.9	-17.2	8.39	...	...	0.00	...	...
NGC3738	nb/d	10	4.9	-17.2	8.62	-1.46	UV,24	0.00	...	...
NGC2537	M	8	6.9	-17.2	9.27	-1.37	UV,24	1.00	...	-1.66
UGCA212	nb/d	8	10.1	-17.2	9.31	...	...	0.00	...	...
NGC3125	nb/d	10	10.8	-17.1	8.95	-0.43	Ha	0.00	...	...
NGC5204	nb/d	9	4.7	-17.0	8.93	-1.20	UV,24	0.00	...	...
UGCA103	P	9	10.4	-17.0	9.06	-2.65	Ha	0.05	0.6 ± 0.5	...
NGC5408	nb/d	10	4.8	-17.0	9.10	-0.97	Ha	0.00	...	...
UGCA106	nb/d	9	9.8	-17.0	9.09	-1.17	UV,24	0.00	...	...
NGC4625	nb/d	9	8.7	-17.0	9.05	-1.21	UV,24	0.00	...	...
NGC2337	nb/d	10	7.9	-17.0	8.58	-1.04	Ha	0.00	...	...
NGC0855	P	-1	9.7	-17.0	9.50	-1.59	UV,24	0.33	1.2 ± 0.2	-1.68
ESO383-G087	nb/d	8	3.5	-16.9	8.86	-1.47	Ha	0.00	...	...
UGC04305	nb/d	10	3.4	-16.9	8.78	-0.84	UV	0.00	...	...
SMC	nb/d	9	0.1	-16.8	8.81	-1.43	Ha	0.00	...	...
NGC1800	nb/d	9	8.2	-16.7	8.71	-1.04	UV	0.00	...	...
UGC07490	nb/d	9	8.4	-16.7	8.97	-1.61	Ha,24	0.00	...	...
ESO435-G016	nb/d	3	9.1	-16.7	9.37	-1.12	UV	0.00	...	...
ESO158-G003	nb/d	9	10.0	-16.7	8.65	...	Ha	0.00	...	...

TABLE 1 — *Continued*

Galaxy Name	Category [a]	T	Dist. (Mpc)	M_B (mag)	$\log(M_{*,total})$ ($M_\odot$)	$\log(\psi_{total})$ ($M_\odot$ yr^{-1})	SFR Method	B/T	Sérsic index	$\log(\psi_{1\ kpc})$ ($M_\odot$ yr^{-1})
NGC0404	C	-1	3.3	-16.6	9.53	-1.99	UV,24	0.16	3.4 ± 1.0	-2.07
NGC3299	nb/d	8	10.4	-16.6	9.54	-1.83	UV,24	0.00	...	...
UGC05151	nb/d	10	10.7	-16.6	8.45	-1.30	Ha	0.00	...	...
UGC07690	nb/d	10	7.7	-16.5	8.74	-1.50	UV,24	0.00	...	...
UGC07690	nb/d	10	7.7	-16.5	8.74	-1.19	UV	0.00	...	...
NGC1510	P	-1	9.8	-16.5	8.86	-1.20	UV,24	0.42	...	...
NGC5608	nb/d	10	10.2	-16.5	7.93	-1.08	UV	0.00	...	...
ESO364-G?029	nb/d	10	7.4	-16.5	8.09	-1.60	Ha	0.00	...	...
IC5152	nb/d	10	2.0	-16.5	8.59	-1.46	UV	0.00	...	...
ESO306-G013	nb/d	3	10.8	-16.4	9.24	...	...	0.00	...	...
IC4870	nb/d	10	9.9	-16.4	8.18	-0.89	UV	0.00	...	...
NGC4288	nb/d	7	7.7	-16.4	8.75	-1.42	UV,24	0.00	...	...
IC5256	nb/d	8	10.8	-16.4	8.06	...	...	0.00	...	...
NGC7518	P	1	10.0	-16.4	9.25	...	...	0.16	...	...
UGC05451	nb/d	10	8.7	-16.3	7.76	-1.52	UV	0.00	...	...
UGC02023	nb/d	10	9.2	-16.3	8.96	-1.14	UV	0.00	...	...
UGC09660	nb/d	4	10.2	-16.3	7.97	-1.36	UV	0.00	...	...
MCG-05-13-004	nb/d	9	6.6	-16.3	8.46	...	...	0.00	...	...
NGC4248	nb/d	3	7.2	-16.2	9.20	-2.15	UV,24	0.00	...	...
UGC07698	nb/d	10	6.1	-16.2	8.56	-1.36	UV	0.00	...	...
UGC00891	nb/d	9	10.8	-16.2	8.74	-1.66	UV	0.00	...	...
NGC4204	nb/d	8	10.4	-16.2	9.07	-1.21	UV,24	0.00	...	...
NGC0221	E	-5	0.8	-16.2	10.02	-1.58	UV,24	1.00	2.8 ± 0.3	...
NGC5264	nb/d	9	4.5	-16.2	8.74	-1.66	UV	0.00	...	...
UGC10736	nb/d	8	9.8	-16.1	7.86	-1.51	UV	0.00	...	...
ESO483-G013	nb/d	-1	10.4	-16.1	8.16	-1.28	UV	0.00	...	...
UGC01865	nb/d	9	9.2	-16.1	8.61	-1.56	UV	0.00	...	...
UGC08201	nb/d	10	4.6	-16.0	8.32	-1.56	UV	0.00	...	...
NGC4707	nb/d	9	7.4	-16.0	8.87	-1.33	UV	0.00	...	...
UGC08188	nb/d	9	4.5	-16.0	8.38	-1.21	UV	0.00	...	...
UGC07608	nb/d	10	7.8	-16.0	8.21	-1.18	UV	0.00	...	...
MCG-03-34-002	nb/d	4	10.2	-16.0	8.35	...	...	0.00	...	...
NGC1522	nb/d	10	9.3	-15.9	8.00	-1.11	UV	0.00	...	...
UGC05829	nb/d	10	7.9	-15.9	8.17	-0.86	UV	0.00	...	...
UGC08313	nb/d	5	8.7	-15.9	7.67	-1.61	UV	0.00	...	...
UGC01176	nb/d	10	9.0	-15.9	8.79	-1.34	UV	0.00	...	...
NGC4080	nb/d	10	6.9	-15.9	7.69	-1.59	UV	0.00	...	...
UGC02259	nb/d	8	9.2	-15.9	8.01	-1.34	Ha	0.00	...	...
ESO119-G016	nb/d	10	9.8	-15.8	7.80	-1.52	UV	0.00	...	...
NGC1705	nb/d	10	5.1	-15.8	7.93	-0.98	UV	0.00	...	...
NGC1592	nb/d	10	10.6	-15.8	7.83	3.00	Ha	0.00	...	...
ESO435-IG020	nb/d	10	9.0	-15.8	8.41	-1.01	Ha	0.00	...	...
ESO486-G021	nb/d	2	8.9	-15.7	7.79	-1.38	UV	0.00	...	...
UGC07774	nb/d	7	7.4	-15.7	7.65	-1.84	UV	0.00	...	...
UGC06161	nb/d	8	10.3	-15.7	7.64	-1.23	UV	0.00	...	...
ESO324-G024	nb/d	10	3.7	-15.7	8.55	-1.71	UV	0.00	...	...
ESO409-IG015	nb/d	6	10.4	-15.6	7.62	-1.33	Ha	0.00	...	...
UGC05889	nb/d	9	9.3	-15.6	8.68	-2.11	Ha	0.00	...	...
UGC04426	nb/d	10	10.3	-15.6	8.27	-1.68	UV	0.00	...	...
UGC07639	nb/d	10	8.0	-15.6	7.74	-1.73	UV	0.00	...	...
UGC04787	nb/d	8	6.5	-15.6	7.37	-1.86	UV	0.00	...	...
UGC05672	nb/d	5	6.3	-15.5	7.44	-2.20	UV	0.00	...	...
ESO245-G005	nb/d	10	4.4	-15.5	9.00	-1.24	UV	0.00	...	...
UGC01104	nb/d	9	7.5	-15.5	8.03	-1.59	UV	0.00	...	...
UGC07719	nb/d	8	9.4	-15.5	7.52	-1.60	UV	0.00	...	...

TABLE 1 — *Continued*

Galaxy Name	Category [a]	T	Dist. (Mpc)	M_B (mag)	$\log(M_{*,\mathrm{total}})$ ($M_\odot$)	$\log(\psi_{\mathrm{total}})$ ($M_\odot$ yr^{-1})	SFR Method	B/T	Sérsic index	$\log(\psi_{1\ \mathrm{kpc}})$ ($M_\odot$ yr^{-1})
UGC01056	nb/d	10	10.3	-15.5	8.11	-1.73	Ha	0.00	...	...
ESO302-G014	nb/d	10	9.6	-15.5	7.29	-1.48	UV	0.00	...	...
UGC09405	nb/d	10	8.0	-15.5	8.09	-2.04	UV	0.00	...	...
UGC06457	nb/d	10	10.2	-15.4	7.61	-1.73	UV	0.00	...	...
NGC5477	nb/d	9	7.7	-15.4	7.88	-1.38	UV	0.00	...	...
ISZ399	nb/d	10	9.0	-15.4	7.88	-1.50	Ha	0.00	...	...
ESO059-G001	nb/d	10	4.6	-15.3	8.67	-2.19	Ha	0.00	...	...
UGC07267	nb/d	8	7.3	-15.3	7.35	-1.99	UV	0.00	...	...
UGC05923	nb/d	0	7.2	-15.3	7.69	-2.05	UV	0.00	...	...
ESO383-G091	nb/d	7	3.6	-15.3	8.01	-3.12	Ha	0.00	...	...
NGC4068	nb/d	10	4.3	-15.2	7.67	-1.87	Ha	0.00	...	...
ESO381-G020	nb/d	10	5.4	-15.2	7.76	-1.70	UV	0.00	...	...
UGC04115	nb/d	10	7.7	-15.2	7.40	-1.63	UV	0.00	...	...
UGC01561	nb/d	10	10.5	-15.2	7.81	-1.44	UV	0.00	...	...
ESO377-G003	nb/d	4	9.2	-15.2	7.83	...	...	0.00	...	...
UGC09497	nb/d	6	10.0	-15.1	7.42	-1.67	UV	0.00	...	...
UGC12713	nb/d	0	7.7	-15.1	8.09	-1.92	UV	0.00	...	...
UGC07949	nb/d	10	9.9	-15.1	7.41	-1.59	UV	0.00	...	...
ESO149-G003	nb/d	10	6.4	-15.1	7.36	-1.79	UV	0.00	...	...
IC4247	nb/d	2	5.0	-15.1	7.80	-2.13	UV	0.00	...	...
CGCG262-028	nb/d	5	6.9	-15.1	7.95	-1.64	UV	0.00	...	...
UGC05692	nb/d	9	4.0	-15.1	8.52	-2.31	UV	0.00	...	...
UGC03860	nb/d	10	7.8	-15.0	7.93	-1.79	UV	0.00	...	...
UGC06900	nb/d	10	7.5	-15.0	8.64	-2.11	UV	0.00	...	...
UGCA319	nb/d	9	7.4	-15.0	8.03	-2.03	UV	0.00	...	...
IC2782	nb/d	8	9.7	-15.0	7.50	...	...	0.00	...	...
UGC07271	nb/d	7	7.8	-15.0	7.21	-1.95	UV	0.00	...	...
UGC05456	nb/d	5	3.8	-15.0	8.00	-1.92	UV	0.00	...	...
UGC03966	nb/d	10	6.8	-15.0	8.18	-1.76	UV	0.00	...	...
UGC07866	nb/d	10	4.6	-14.9	7.73	-1.66	UV	0.00	...	...
SBS1331+493	nb/d	10	9.3	-14.9	6.76	-1.85	Ha	0.00	...	...
UGC00695	nb/d	6	10.2	-14.9	7.46	-1.74	UV	0.00	...	...
UGC02014	nb/d	10	9.2	-14.9	7.72	-2.38	UV	0.00	...	...
ESO104-G044	nb/d	9	8.4	-14.9	7.57	-1.75	Ha	0.00	...	...
NGC5238	nb/d	8	5.2	-14.9	7.51	-1.77	UV	0.00	...	...
UGC04998	nb/d	10	10.5	-14.9	8.16	-1.89	UV	0.00	...	...
NGC5229	nb/d	7	5.1	-14.9	8.18	-1.94	UV	0.00	...	...
UGC07916	nb/d	10	8.2	-14.9	7.34	-1.60	UV	0.00	...	...
UGCA153	nb/d	10	6.5	-14.9	7.84	-2.05	UV	0.00	...	...
UGCA298	nb/d	-1	10.3	-14.9	7.15	...	...	0.00	...	...
UGC07599	nb/d	8	6.9	-14.9	7.85	-1.89	UV	0.00	...	...
UGC09893	nb/d	7	10.9	-14.9	7.28	-1.71	UV	0.00	...	...
ESO249-G036	nb/d	10	9.6	-14.8	7.05	-1.64	UV	0.00	...	...
UGC05453	nb/d	10	9.3	-14.8	7.29	-2.80	Ha	0.00	...	...
UGC05288	nb/d	8	6.8	-14.8	7.65	-1.76	UV	0.00	...	...
UGC05139	nb/d	10	3.8	-14.8	7.56	-1.81	UV	0.00	...	...
ESO104-G022	nb/d	10	8.7	-14.8	7.96	-1.82	Ha	0.00	...	...
KUG1004+392	nb/d	10	7.8	-14.8	7.10	-1.88	UV	0.00	...	...
UGC07577	nb/d	10	2.7	-14.8	8.00	-2.19	UV	0.00	...	...
UGC02716	nb/d	8	6.2	-14.7	8.67	-1.97	UV	0.00	...	...
UGC05740	nb/d	9	9.3	-14.7	7.29	-1.55	UV	0.00	...	...
UGC07678	nb/d	6	9.3	-14.7	6.88	-1.37	UV	0.00	...	...
UGC03817	nb/d	10	8.6	-14.7	8.05	-2.05	Ha	0.00	...	...
UGC07559	nb/d	10	4.9	-14.7	7.65	-1.79	UV	0.00	...	...
UGC09992	nb/d	10	8.6	-14.7	7.70	-1.84	UV	0.00	...	...

TABLE 1 — *Continued*

Galaxy Name	Category [a]	T	Dist. (Mpc)	M_B (mag)	$\log(M_{*,total})$ ($M_\odot$)	$\log(\psi_{total})$ ($M_\odot$ yr^{-1})	SFR Method	B/T	Sérsic index	$\log(\psi_{1\ kpc})$ ($M_\odot$ yr^{-1})
UGC07950	nb/d	10	7.9	-14.6	7.20	-1.48	UV	0.00	...	...
CGCG217-018	nb/d	10	8.2	-14.6	7.14	-1.89	UV	0.00	...	...
UGC07242	nb/d	6	5.4	-14.6	7.26	...	...	0.00	...	...
ESO325-G011	nb/d	10	3.4	-14.6	7.88	-1.91	Ha	0.00	...	...
UGC09211	nb/d	10	10.7	-14.6	7.75	-1.39	UV	0.00	...	...
MCG-04-02-003	nb/d	9	9.8	-14.6	7.20	-2.20	Ha	0.00	...	...
ESO252-IG001	nb/d	99	6.0	-14.5	7.62	-2.42	Ha	0.00	...	...
UGC05797	nb/d	10	6.8	-14.5	7.24	-2.14	UV	0.00	...	...
UGCA281	nb/d	10	5.7	-14.5	6.82	-1.41	Ha	0.00	...	...
UGC05423	nb/d	10	5.3	-14.4	7.75	-2.33	UV	0.00	...	...
UGC05373	nb/d	10	1.4	-14.4	7.90	-2.29	UV	0.00	...	...
UGC05427	nb/d	8	7.1	-14.3	6.90	-1.92	UV	0.00	...	...
UGC06102	nb/d	10	8.5	-14.3	7.22	-1.89	UV	0.00	...	...
ESO553-G046	nb/d	1	5.0	-14.3	7.39	...	...	0.00	...	...
KUG1413+573	nb/d	10	7.4	-14.3	7.03	-2.32	UV	0.00	...	...
UGC00685	nb/d	9	4.7	-14.3	7.62	-2.19	UV	0.00	...	...
UGC05076	nb/d	10	8.3	-14.3	7.15	-2.91	Ha	0.00	...	...
ESO140-G019	nb/d	10	10.8	-14.3	7.63	-1.75	Ha	0.00	...	...
UGC05918	nb/d	10	7.4	-14.3	7.67	-1.95	UV	0.00	...	...
UGC08024	nb/d	10	4.3	-14.3	7.52	-1.81	UV	0.00	...	...
UGC08683	nb/d	10	9.6	-14.3	7.00	-1.57	UV	0.00	...	...
UGC00668	nb/d	10	0.7	-14.2	8.00	-2.09	UV	0.00	...	...
ESO238-G005	nb/d	10	8.9	-14.2	7.01	-1.81	UV	0.00	...	...
NGC6789	nb/d	10	3.6	-14.2	7.36	-2.43	Ha	0.00	...	...
IC4316	nb/d	10	4.4	-14.2	7.89	...	...	0.00	...	...
MRK36	nb/d	10	7.8	-14.1	7.09	-1.43	Ha	0.00	...	...
UGC09240	nb/d	10	2.8	-14.1	7.46	-2.24	UV	0.00	...	...
ESO300-G016	nb/d	10	7.8	-14.1	7.01	-2.28	UV	0.00	...	...
UGC06541	nb/d	10	3.9	-14.1	7.36	-2.08	Ha	0.00	...	...
NGC4190	nb/d	10	3.5	-14.0	7.08	-1.99	UV	0.00	...	...
AM0704-582	nb/d	9	4.9	-14.0	7.62	-2.23	Ha	0.00	...	...
UGC02684	nb/d	10	6.5	-13.9	8.12	-2.19	UV	0.00	...	...
ESO473-G024	nb/d	10	8.0	-13.9	6.98	-2.05	UV	0.00	...	...
IC2787	nb/d	6	7.7	-13.9	6.87	-4.84	Ha	0.00	...	...
MCG+07-26-012	nb/d	6	6.4	-13.9	6.72	-3.07	Ha	0.00	...	...
ESO348-G009	nb/d	10	8.6	-13.9	6.88	-1.77	UV	0.00	...	...
AM0605-341	nb/d	10	7.0	-13.9	7.38	-1.98	Ha	0.00	...	...
UGC07007	nb/d	9	10.1	-13.8	6.93	-1.90	UV	0.00	...	...
UGC05336	nb/d	10	3.7	-13.8	7.51	-1.99	UV	0.00	...	...
UGCA290	nb/d	10	6.7	-13.8	6.86	-1.83	UV	0.00	...	...
IC0559	nb/d	5	4.9	-13.8	7.03	-2.37	UV	0.00	...	...
ESO444-G084	nb/d	10	4.6	-13.7	7.20	-2.21	UV	0.00	...	...
MCG+07-26-011	nb/d	8	6.0	-13.7	6.64	-2.76	Ha	0.00	...	...
UGC08245	nb/d	10	3.6	-13.7	6.89	-2.60	UV	0.00	...	...
UGC07605	nb/d	10	4.4	-13.7	6.92	-2.16	UV	0.00	...	...
ESO384-G016	nb/d	10	4.5	-13.7	7.36	-4.66	Ha	0.00	...	...
UGC05917	nb/d	10	10.3	-13.7	7.17	-1.74	UV	0.00	...	...
MRK475	nb/d	10	9.0	-13.7	7.16	-1.62	Ha	0.00	...	...
UGC10669	nb/d	10	9.2	-13.7	6.99	-2.53	UV	0.00	...	...
UGC08638	nb/d	10	4.3	-13.6	6.67	-2.25	UV	0.00	...	...
UGC06456	nb/d	10	4.3	-13.6	6.75	-1.92	UV	0.00	...	...
SextansA	nb/d	10	1.3	-13.6	7.52	-1.92	UV	0.00	...	...
UGC07584	nb/d	9	7.3	-13.6	6.84	-2.22	UV	0.00	...	...
CGCG035-007	nb/d	5	5.2	-13.5	7.51	-2.51	UV	0.00	...	...
UGC12894	nb/d	10	8.2	-13.5	7.63	...	...	0.00	...	...

TABLE 1 — *Continued*

Galaxy Name	Category [a]	T	Dist. (Mpc)	M_B (mag)	$\log(M_{*,total})$ ($M_\odot$)	$\log(\psi_{total})$ ($M_\odot$ yr^{-1})	SFR Method	B/T	Sérsic index	$\log(\psi_{1\ kpc})$ ($M_\odot$ yr^{-1})
UGC04459	nb/d	10	3.6	-13.4	7.21	-2.16	Ha	0.00	...	...
NGC3741	nb/d	10	3.2	-13.4	6.89	-2.23	Ha	0.00	...	...
UGC08651	nb/d	10	3.0	-13.4	6.63	-2.42	UV	0.00	...	...
NGC4163	nb/d	10	3.0	-13.3	6.99	-2.34	UV	0.00	...	...
UGC08308	nb/d	10	4.2	-13.2	6.52	-2.42	UV	0.00	...	...
KUG1207+367	nb/d	10	4.5	-13.1	6.76	-2.71	UV	0.00	...	...
UGC07356	nb/d	10	6.7	-13.1	6.88	...	...	0.00	...	...
LSBCD564-08	nb/d	10	8.7	-13.1	6.71	-4.43	Ha	0.00	...	...
UGC08508	nb/d	10	2.7	-13.1	7.11	-2.77	Ha	0.00	...	...
UGC04483	nb/d	10	3.2	-13.0	6.68	-2.41	UV	0.00	...	...
LSBCD565-06	nb/d	10	9.1	-13.0	6.88	-4.79	Ha	0.00	...	...
KDG61	nb/d	8	3.6	-12.9	8.08	-3.21	UV	0.00	...	...
AndIV	nb/d	10	6.1	-12.9	6.93	-2.52	UV	0.00	...	...
LEDA166137	nb/d	10	6.0	-12.9	6.42	-2.41	UV	0.00	...	...
UGC08055	nb/d	10	6.6	-12.9	6.45	-2.17	UV	0.00	...	...
BTS76	nb/d	10	6.0	-12.9	6.58	-3.63	UV	0.00	...	...
UGC05209	nb/d	10	6.4	-12.8	6.59	-2.76	UV	0.00	...	...
UGCA438	nb/d	10	2.2	-12.8	6.25	-2.57	UV	0.00	...	...
LEDA100404	nb/d	9	6.8	-12.7	6.73	-4.92	Ha	0.00	...	...
UGC07298	nb/d	10	4.2	-12.7	6.45	...	...	0.00	...	...
UGC09128	nb/d	10	2.2	-12.7	6.66	-2.98	UV	0.00	...	...
KKH34	nb/d	10	4.6	-12.6	8.54	-3.95	Ha	0.00	...	...
UGC08091	nb/d	10	2.1	-12.6	6.68	-2.58	UV	0.00	...	...
CGCG269-049	nb/d	10	3.2	-12.4	6.54	-2.80	UV	0.00	...	...
UGC08833	nb/d	10	3.2	-12.4	6.35	-2.75	UV	0.00	...	...
UGC05428	nb/d	10	3.5	-12.4	7.42	-4.58	Ha	0.00	...	...
UGC08215	nb/d	10	4.6	-12.4	6.28	-2.88	UV	0.00	...	...
LSBCF573-01	nb/d	10	7.2	-12.4	6.35	-4.69	Ha	0.00	...	...
LSBCD634-03	nb/d	10	9.5	-12.1	6.60	-4.45	Ha	0.00	...	...
SDSSJ0825+3532	nb/d	10	9.3	-12.0	6.66	-2.25	Ha	0.00	...	...
ESO349-G031	nb/d	10	3.2	-12.0	6.14	-5.10	Ha	0.00	...	...
KKH37	nb/d	10	3.4	-12.0	6.70	-3.10	UV	0.00	...	...
UGCA276	nb/d	10	3.2	-11.9	6.17	...	...	0.00	...	...
UGC12613	nb/d	10	0.8	-11.9	7.60	-3.49	UV	0.00	...	...
UKS1424-460	nb/d	10	3.6	-11.8	6.51	-3.59	Ha	0.00	...	...
UGCA292	nb/d	10	3.1	-11.8	6.04	-2.76	UV	0.00	...	...
DDO210	nb/d	10	0.9	-11.6	6.26	-3.80	UV	0.00	...	...
UGC05364	nb/d	10	0.7	-11.6	6.48	-3.28	UV	0.00	...	...
UGC05272b	nb/d	10	7.1	-11.6	6.45	-2.80	UV	0.00	...	...
UGCA20	nb/d	10	9.0	-11.4	7.56	-1.77	UV	0.00	...	...
KDG73	nb/d	10	3.7	-11.0	5.69	-5.47	Ha	0.00	...	...
LEDA166115	nb/d	-1	4.5	-9.8	6.36	-5.41	Ha	0.00	...	...
ESO245-G007	nb/d	10	0.4	-9.7	6.36	...	...	0.00	...	...
BK3N	nb/d	10	4.0	-9.6	5.75	-5.46	Ha	0.00	...	...
M81dwA	nb/d	10	3.6	-9.2	5.47	-5.20	Ha	0.00	...	...
KKR03	nb/d	10	2.1	-8.9	6.59	-5.68	Ha	0.00	...	...
LGS3	nb/d	99	0.6	-7.9	5.94	-6.90	Ha	0.00	...	...
LeoT	nb/d	10	0.4	-6.9	4.57	-5.92	Ha	0.00	...	...

[a] E – Elliptical Galaxy; C – Classical bulge; P – Pseudobulge; nb/d – no bulge/dwarf; M – advanced stage merger
[b] NGC 5194 & NGC 5195 are currently interacting.
[c] Categorized as classical bulge due to Sérsic index despite nuclear morphology
[d] Morphology strongly indicates pseudobulge, despite high Sérsic index